Thermodynamics and structure behavior of a confined binary mixture by Reactive Monte Carlo simulations

H. Domínguez

Instituto de Investigaciones en Materiales, Universidad Nacional Autónoma de México,
México, D.F. 04510
e-mail: hectordc@servidor.unam.mx

Adsorption and structure of a confined binary mixture is investigated with Reactive Monte Carlo (RxMC) simulations. This method allowed us to study thermodynamics of the system at different temperatures and at different pore sizes at chemical equilibrium imposed by the reaction A $\rightleftharpoons$ B. In particular studies of equilibrium composition as a function of particle interactions between particles of the same specie and cross interactions between particles of different species were investigated . As a pore model it was used the slit-like geometry where it was observed that at very narrow pores the particle composition departed from that in the bulk. The results also showed that the creation of particles was determined not only by the strength of the particle-particle interactions but also by the wall-particle interactions. In fact, it was possible to enhance creation of a specific specie in the mixture by changing the affinity of the walls to that particular specie.

Keywords: Confined mixture; Reactive Monte Carlo; particle interactions.

La adsorción y la estructura una mezcla binaria confinada fue investigada mediante simulaciones de Monte Carlo Reactivo. Este método nos permitio hacer estudios de la termodinámica del sistema a diferentes temperaturas en diferentes tamaños de poro en equilibrio químico determinado por la reacción A $\rightleftharpoons$ B. En particular estudios de composiciones en equilibrio fueron investigadas como función de la interacción entre partículas de la misma especie y de diferentes especies. El modelo de poro que se uso consistio de dos placas paralelas y se observó que para poros muy angostos la composición de partículas se alejaba de los datos en el bulto. Los resultados también mostraron que la creación de partículas estuvo determinada no solo por la interacción partícula-partícula si no también por interacción pared-partícula. Finalmente, se observo que la creacón de partículas se puede incrementar haciendo que las paredes favorescan mas la interacción con ciertas partículas del sistema.

Descriptores: Mezcla confinada; Monte Carlo Reactivo; interacciones de partículas.

PACS: 61.20.Ja; 61.30.Hn; 68.08.De

1. Introduction

Nowadays it is well known that when fluids are confined in narrow pores their properties are modified from those in bulk. The new wall-fuid interactions can alter not only the structure and dynamic properties of the fluids but also can have significant influence on the fluids phase behavior. In fact several studies have been carried out from experimental [1–4], theoretical [5–7] and computational [8–13] point of view to study these phenomena. In particular computer simulations have proved to be a powerful tool to investigate such systems, where people have used Molecular dynamics [14, 15] and Monte Carlo [13, 16] techniques to investigate not only one component fluids [13, 17] but also mixtures [8–11]. In fact, different Monte Carlo ensambles have been used, NVT, NPT and μ VT to study bulk and confined fluids, however, few years ago the Reactive Monte Carlo (RxMC) appeared [18] as a different approach to study systems where chemical reactions were involved. For confined fluids just few works have adreseed the problem with this RxMC method [18–22]. For instance people have used RxMC to study the 2NO $\rightleftharpoons$ (NO)$_2$ reaction in slit pores [20] whereas other authors have [19] conducted studies to investigate dimerization under confinement using the RxMC methodology. For recent good reviews of RxMC simulations, in bulk and in confinement, the reader can see references [23, 24].

It is commun to use Gran Canonical or Semi Gran canonical Monte Carlo simulations in slit pores systems, however, it is necessary to know the equilibrium chemical potential as input which some times it is not an available information. On the other hand, these ensambles present problems to conduct simulations at high densities. Therefore in the present simulations we use RxMC, firstly because even when the chemical potencial is unknown the system finds its natural chemical equilibrium, *i.e.* we conduct simulations of the chemical reaction directly. On the other hand we will still explore the benefits of using RxMC in confined fluids, *i.e.* we study a binary mixture composed of "A" and "B" particles confined in a slit-pore, however, we focused on the effects of the cross interaction between the different particles with symmetric and antisymmetric walls on the behavior of confined mixtures since not much work have been carried out in this direction.

2. Computational Method and Model

The binary mixture of "A"and "B" particles was prepared by conducting the chemical reaction A $\rightleftharpoons$ B. It is important to mention that this is not a straightforward chemical reaction observed in nature, however, this simple model allowed us to prepare the binary system at equilibrium composition. More

over, the advantage of using this model is that we studied adsorption of particles at conditions where the system reached its chemical equilibrium.

Then, simulations for the A $\rightleftharpoons$ B chemical reaction confined in a slit pore were conducted using the Reactive Monte Carlo method in the NPT ensemble [25], however, the pressure was imposed only in the X-Y directions so the separation between the two walls was always constant.

The initial configuration was started from a random number of "A" and "B" particles located in a simulation box. Then, all particles were confined by two parallel walls separated by a distance H and the simulations started.

We do not intent to give explicit details of the RxMC (the reader can see *e.g.* references [18] for full details) and we only show the principal steps of the method for our simulations.

1. A random particle is chosen from "A" or "B" particles and a change in position is attempted with the standard MC probability [25].

2. A random change in the X-Y area is attempted to keep constant pressure an it is accepted with the usual MC probability [25].

3. A forward reaction step is attempted, *i.e.* a random particle "A" is chosen and it is changed to a "B" particle. Then, the move is accepted with probability of min[1, $P_{r \to s}$].

4. A reverse reaction step is attempted, *i.e.* a particle "B" is chosen at random and it is changed to an "A" particle. Then, the move is accepted with probability of min[1, $P_{s \to r}$].

Here, the transition probability for a reaction in the direction $r \to s$ is given by:

$$P_{r \to s} = \exp(-\beta \delta U_{rs}) \prod_{i=1}^{C} q_i^C \prod_{i=1}^{C} \frac{N_i!}{[N_i + \nu_i]!} \quad (1)$$

$\beta \delta U_{rs}$ is the energy change from state r to s, q_i is the partition function, N_i is the number of particles of type i, ν is the stoichiometric coefficient and C is the number of components [18]. The transition probability for a reaction in the reverse direction ($s \to r$) can generated by replacing ν_i by $-\nu_i$

All particle-particle interactions were given by the Lennard-Jones potential with equal particle diameters for both species.

$$u(r_{ij}) = 4\epsilon_{ij} \left[\left(\frac{\sigma_{ij}}{r} \right)^{12} - \left(\frac{\sigma_{ij}}{r} \right)^{6} \right] \quad (2)$$

with σ_{ij} and ϵ_{ij} the Lennard Jones parameters and the index i, j referred to "A" or "B" particles. For the slit pore continuous planar walls were used where the particle-wall interaction was given by a 9-3 potential,

$$u_w(r) = \epsilon_w \left[\frac{2}{45} \left(\frac{\sigma_{wm}}{r} \right)^{9} - \frac{1}{3} \left(\frac{\sigma_{wm}}{r} \right)^{3} \right] \quad (3)$$

with $\epsilon_w = 2\pi\epsilon_{wm}\sigma_{wm}^3\rho_w$, ρ_w is the wall density. The subindex m refers to the "A" or "B" specie. For the simulations we used $\sigma_{wA} = \sigma_{wB} = 0.9934\,\sigma_{ar}$ and $\rho_w\sigma_{ar}^3 = 4.5$, σ_{ar} and ϵ_{ar} are the argon parameters so that the values were chosen to mimic a fluid of argon in graphite walls.

Then, three pore widths were investigated, H = $10\sigma_{AA}$, $5\sigma_{AA}$ and $3\sigma_{AA}$ with a total of 1000, 800 and 600 particles respectively, using periodic boundary conditions as usual in the X-Y directions only. Finally, simulations were conducted in reduced units (using the argon parameters) as the usual way, *e.g.* H* = H/σ_{ar}, $\epsilon_{wB}^* = \epsilon_{wB}/\epsilon_{ar}$, etc. [25].

For the rest of the paper all quantities are given in reduced units and they are written without the superindex. In all simulations the reduced pressure was P = 1.0. Then, the systems were equilibrated for 10000 Monter Carlo steps and another 60000 steps were run for data production. Few simulations were also run up to 100000 to see any variations, however, we did not observe significant changes in the results.

3. Results

In this section results for the slit-pores simulations were investigated. The effects of the reaction as a function of temperature, particle-particle and particle-wall interactions were analyzed.

3.1. Temperature effects

To study the temperature effects, firstly the cross energy interaction between particles of different specie was fixed at
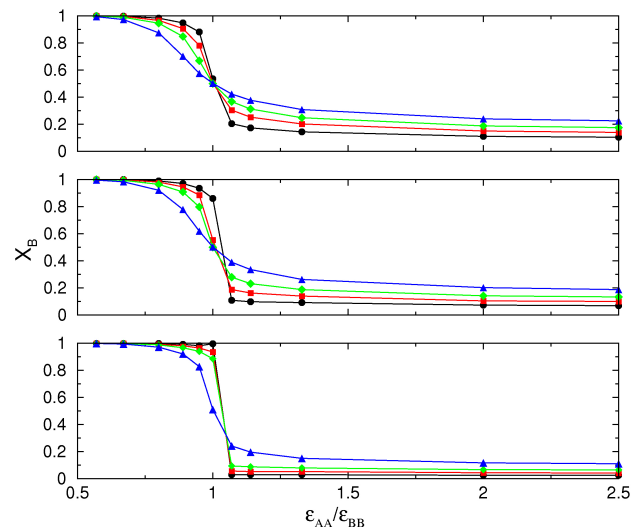

FIGURE 1. Concentration number of "B" (X_B) particles as a function of the $\epsilon_{AA} / \epsilon_{BB}$ parameter at different pore sizes and at different temperatures. Black circles represent data for the bulk system, square reds are data for a reduced pore width of Z = 10, green diamonds for Z = 5 and blue tringles for Z = 3. Top figure are the results given at reduced temperature of T = 1.5, middle at T = 1.4 and bottom at T = 1.2. In all figures $\epsilon_{AA} = 1.0$ and $\epsilon_{AB} = 0.5$. Solid lines are just to guide the eyes.
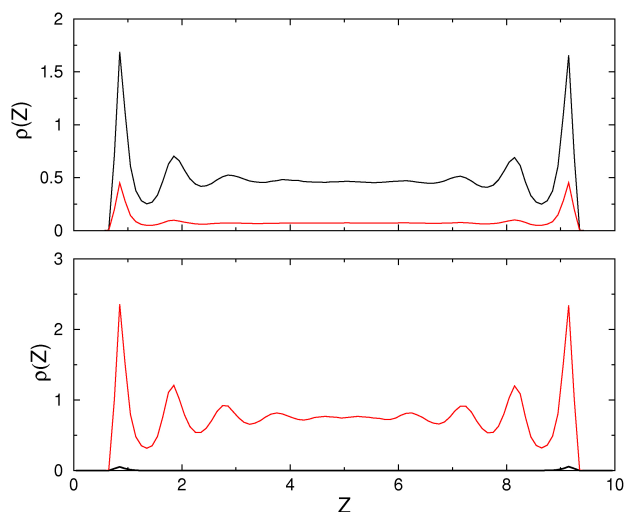
FIGURE 2. Density profiles at reduced temperature T = 1.5 and at reduced pore size Z = 10. Top figure is for $\epsilon_{AA}/\epsilon_{BB}$ = 2.0 and bottom figure is for $\epsilon_{AA} / \epsilon_{BB}$ = 0.666. Black lines represent the profiles for "A" particles and red lines for "B" particles. In all cases ϵ_{AA} = 1.0 and ϵ_{AB} = 0.5.

FIGURE 3. Phase diagrams of temperature as a function of particle concentration, X_B. Top figure is for $\epsilon_{AA}/\epsilon_{BB}$ = 0.95, middle figure for $\epsilon_{AA}/\epsilon_{BB}$ = 1.0 and bottom figure for $\epsilon_{AA}/\epsilon_{BB}$ = 1.07. In all cases ϵ_{AA} = 1.0 and ϵ_{AB} = 0.5. Colors are the same as in Fig. 1. Solid lines are just to guide the eye.

ϵ_{AB} = 0.5 and symmetric walls were used for the simulations, *i.e.* $\epsilon_{wA} = \epsilon_{wB}$ = 0.4834.

For these simulations different reduced pore widths were considered (H = 10, 5 and 3) and reaction of the particles were studied as a function of the particle interaction, *i.e.* the energy ratio $\epsilon_{AA}/\epsilon_{BB}$. In Fig. 1 the ratio of the final average number of particles of specie "B", X_B, (= N_B/N_T where N_T is the number of total particles) is plotted for different values of temperature.

Since in reduced units ϵ_{AA} = 1.0, then large values of $\epsilon_{AA}/\epsilon_{BB}$ means small ϵ_{BB} whereas small values of $\epsilon_{AA}/\epsilon_{BB}$ means large ϵ_{BB}. For weak "B" interactions ($\epsilon_{BB} < \epsilon_{AA}$) it was observed large number of particles "A" (small number of particles "B"), *i.e.* "A" particles were favored in the reaction. As the "BB" interaction increased ($\epsilon_{AA}/\epsilon_{BB}$ decreased) the reaction to "B" was more favorable and consequently the number of "B" particles increased as observed by the plots in Fig. 1. The same trends were depicted from all temperatures and for all pore widths. Actually, as the pore size increased the X_B values approached to those of the bulk system as it was expected. It is also important to note that the change from low to high X_B became sharper as the temperature decreased.

The structure of the fluids were analyzed in terms of their density profiles and they were plotted in Fig. 2 for two $\epsilon_{AA}/\epsilon_{BB}$ ratios at one single temperature. For weak "BB" particle interactions the density profiles of component "B" behaved like a gas in the middle of the box whereas the "A" particles formed layers close to the walls with a bulk liquid in the middle of the box. On the other hand, for a strong "BB" interaction we observed that "B" particles were well adsorbed on the surfaces by forming layers trough all the pore whereas just few "A" particles were depicted close to the walls.
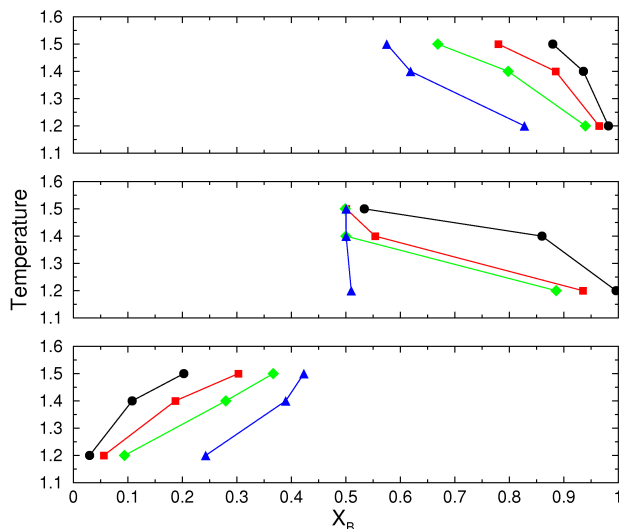
As stated before, it is well known that the phase diagram of confined systems is modified, therefore we studied these diagrams to observe how they changed from that of the bulk in all our systems. In Fig. 3 diagrams of temperature as a function of the particle fraction of component "B" are shown at different interactions. It was possible to observe that for strong "BB" interactions ($\epsilon_{AA}/\epsilon_{BB} < 1$) the pore was rich in "B" particles. Interesting was to see the data shifted to the left from the bulk as the pore width became narrow. On the other hand, for weak "BB" interactions ($\epsilon_{AA}/\epsilon_{BB} > 1$) the system was rich in "A" particles, *i.e.* there was low concentration of "B" particles. In this case, it was observed that the data were shifted to the right from those in the bulk as the pore became narrow. However, for any value of the "BB" interaction the data approached to the bulk as the size of the pore increased as expected.

3.2. Different ϵ_{AB} interaction

All above simulations were conducted for a cross interaction of ϵ_{AB} = 0.5. However, when this interaction was increased different features were observed. Firstly, to study how the particles were structured inside the pore we analyzed the density profiles, and in Fig. 4 we show typical plots for a system with ϵ_{AB} = 1.25 at reduced temperature of T=1.5 in the pore size Z = 10 for two "BB" interactions, $\epsilon_{AA}/\epsilon_{BB}$ = 0.666 (top) and $\epsilon_{AA}/\epsilon_{BB}$ = 2.0 (bottom). As in Fig. 2 we saw that small $\epsilon_{AA}/\epsilon_{BB}$ produced more number of "B" particles (with strong structure close to the walls) than "A" particles, however, since in this case ϵ_{AB} was stronger than that in Fig. 2, there were here more "A" particles with stronger structure.

More over, in this case, "B" particles liked to be with "A" particles and consequently it was more difficult to form rich phases composed only of "A" or "B" particles as indicated in
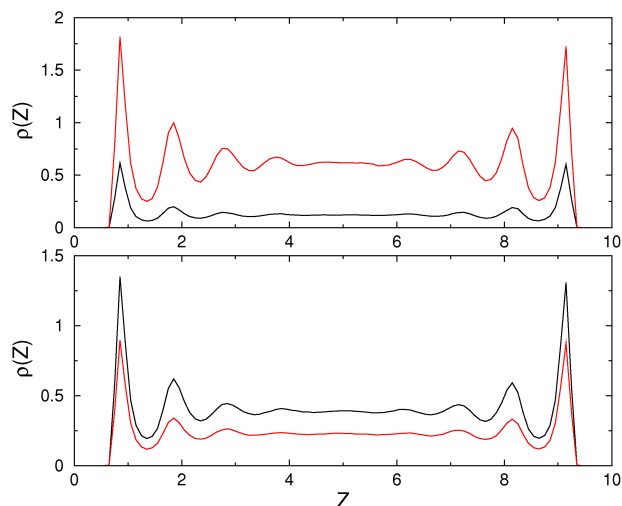
FIGURE 4. Density profiles at reduced temperature T = 1.5 and at reduced pore size Z = 10. Top figure is for $\epsilon_{AA}/\epsilon_{BB} = 0.666$ and bottom figure is for $\epsilon_{AA}/\epsilon_{BB} = 2.0$. Black lines represent the profiles for "A" particles and red lines for "B" particles. In all cases $\epsilon_{AA} = 1.0$ and $\epsilon_{AB} = 1.25$.
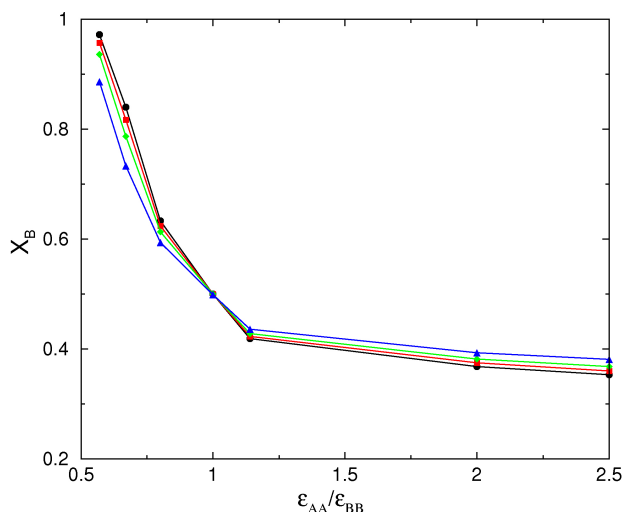

FIGURE 5. Concentration number of "B" (X_B) particles as a function of the $\epsilon_{AA}/\epsilon_{BB}$ at reduced temperature of T = 1.5. Black circles represent data for the bulk system, square reds are data for a reduced pore width of Z = 10, green diamonds for Z = 5 and blue tringles for Z = 3. In the figure $\epsilon_{AA} = 1.0$ and $\epsilon_{AB} = 1.25$. Solid lines are just to guide the eye.

Fig. 4. As in the previous results, it was observed that $\epsilon_{AA}/\epsilon_{BB} < 1$ present higher concentration of "B" than "A" particles. In fact, due to the high concentration of "B" particles in the fluid they showed high structure as indicated by the oscillations in the profile. For $\epsilon_{AA}/\epsilon_{BB} > 1$ there were more "A" than "B" particles, altought, the diference in the number of particles between the two species was small (Fig. 4b) compared with that in Fig. 2.

When concentration of "B" particles was plotted as a function of $\epsilon_{AA}/\epsilon_{BB}$ parameter different features were observed. In contrast with Fig. 1, in this case more continuos

increments of "B" particles as the "BB" interaction increased was observed (Fig. 5). Due to the large value of ϵ_{AB} there was a competition between "AB" and "AA" particle interactions which made formation of "B" particles a more continuous process than that observed above (see Fig. 1).

As it was also expected, formation of "B" particles was closer to the bulk as the pore width became wider.

3.3. Walls more attractive to one component ("B" particles)

When walls favored the interaction to one particular component different features were also observed. Figure 6 shown a system where the wall-"A" particles interactions were stronger than the wall-"A" particles interactions by using $\epsilon_{AB} = 1.25$. In this case the attraction between "B" particles and the walls ($\epsilon_{wB} = 0.9668$) was twice stronger than that between the "A" particles and the walls ($\epsilon_{wA}=0.4834$). Due to these interactions, in this case, there were always more "B" particles than "A" particles regardless the $\epsilon_{AA}/\epsilon_{BB}$ interaction except for the $\epsilon_{AA}/\epsilon_{BB} = 2.0$ and 2.5 at the pore size Z=10. It was also interested to see (Fig. 6) that we did not observe a crossover at $\epsilon_{AA}/\epsilon_{BB} = 1$. However, this can be explained considering that the walls helped to form more "B" than "A" particles leading only few proportion of "A" particles in the pore. In most of the cases it was observed less than 50% of "A" particles in the simulation boxes.

3.4. A wall attractive to "A" particles and the other wall attractive to "B" particles

Finally a last study was carried out to investigate how the pore walls affect the formation of "A" or "B" particle during
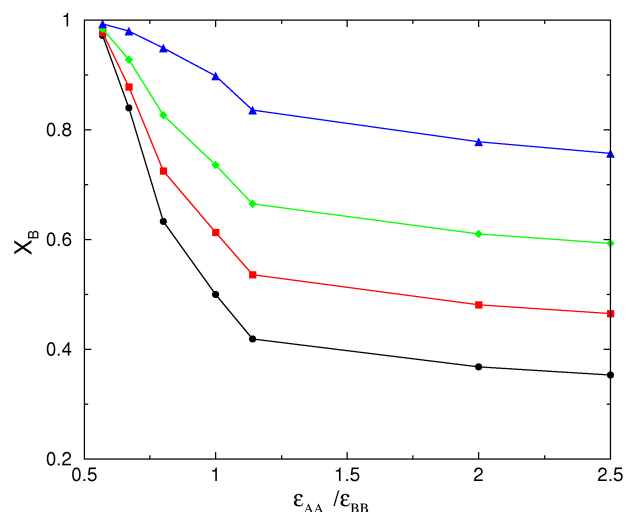

FIGURE 6. Concentration number of "B" (X_B) particles as a function of the $\epsilon_{AA}/\epsilon_{BB}$ at reduced temperature of T = 1.5. In this plot the wall are more attractive to "B" particles than "A" particles, $\epsilon_{WA} = 0.4834$ and $\epsilon_{WB} = 0.9668$. Black circles represent data for the bulk system, square reds for a reduced pore width of Z = 10, green diamonds for Z = 5 and blue tringles for Z = 3. $\epsilon_{AA} = 1.0$ and $\epsilon_{AB} = 1.25$. Solid lines are just to guide the eye.

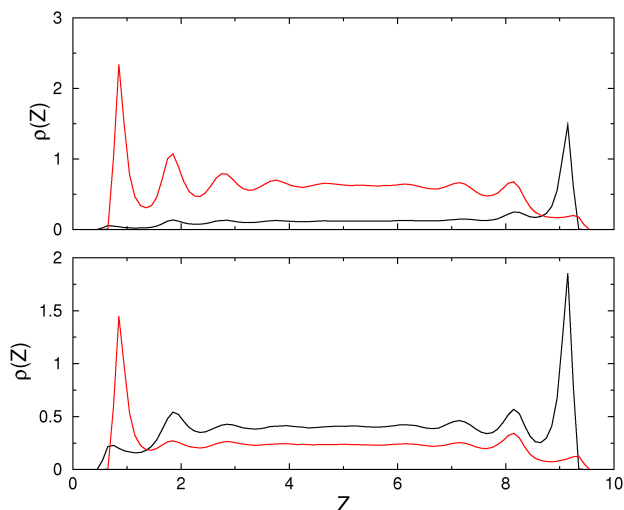FIGURE 7. Density profiles at reduced temperature T = 1.5 and at a reduced pore size Z = 10. In this figures one wall was attractive to "A" particles whereas the other wall was attractive to "B" particles. Top figure is for $\epsilon_{AA}/\epsilon_{BB} = 0.666$ bottom figure is for $\epsilon_{AA}/\epsilon_{BB} = 2.0$. Black lines represent the profile for "A" particles and red lines for "B" particles. In all cases $\epsilon_{AA} = 1.0$ and $\epsilon_{AB} = 1.25$.
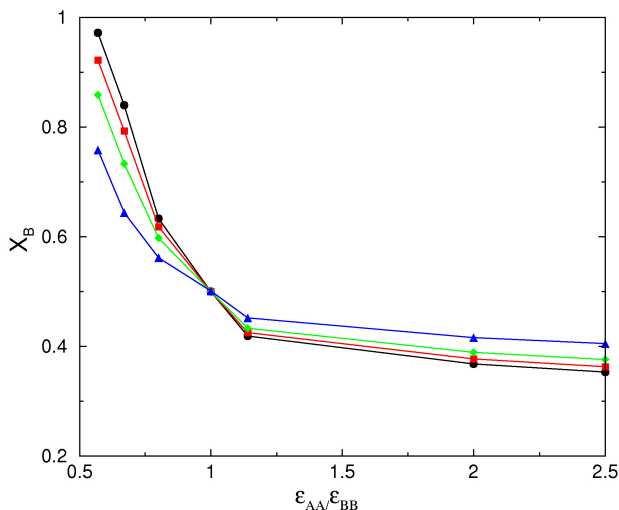

FIGURE 8. Concentration number of B (X_B) particles as a function of the $\epsilon_{AA}/\epsilon_{BB}$ at reduced temperature of T = 1.5. In this figures one wall was attractive to "A" particles whereas the other wall was attractive to "B" particles. Black circles represent data for the bulk system, square reds for a reduced pore width of Z = 10, green diamonds for Z = 5 and blue tringles for Z = 3. $\epsilon_{AA} = 1.0$ and $\epsilon_{AB} = 1.25$. Solid lines are just to guide the eye.

a reaction when one specie of particles was attracted to one wall whereas the other wall attracted the other specie.

From Fig. 7, density profiles for a pore width $Z = 10$ at different $\epsilon_{AA}/\epsilon_{BB}$ ratios are shown. It was observed that "A" particles were adsorbed to one wall while "B" particles to the other. As it was expected for $\epsilon_{AA} < \epsilon_{BB}$ there were more "B" particles through the pore (see top of Fig. 7). More over, the "B" particles developed several adsorbed layers close to one of the walls and at the same time the other wall was satu-

rated mainly by "A" particles. When $\epsilon_{AA} > \epsilon_{BB}$ there were similar number of "A" and "B" particles in the pore, nevertheless, there were still "B" particles adsorbed to one wall whereas "A" particles were adsorbed to the other wall, however, in this case the particles formed more structured layers as it shown in the bottom plot of Fig. 7. In this case, it is interesting to observe a few "A" particles even next to the selective wall to "B" particles. However, this can be understood in terms of the cross interactions. Since the cross parameter ($\epsilon_{AB} = 1.25$) favored the "A" and "B" interaction then we found few "A" particles close to "B" particles. On the other hand the "AA" interaction is stronger than the "BB" therefore the probability to find "A" particles next to "B" particles is higher in regions of high "B" concentrations.

The concentration plots as a function of particle interaction is shown in Fig. 8. Basically, the same trend was observed as previous cases, *i.e.* small $\epsilon_{AA}/\epsilon_{BB}$ values made larger X_B whereas large values of $\epsilon_{AA}/\epsilon_{BB}$ produced small X_B. Since, there was a competition between "A" and "B" particles the crossover at $\epsilon_{AA}/\epsilon_{BB} = 1.0$ was observed once again.

4. Conclusions

We present results of a binary mixture confined in two parallel walls by using the Reactive Monte Carlo method. This technique allowed us to study adsorption of the fluids at chemical equilibrium conditions. In particular we investigated how fluids under confinement were affected by the interactions between particles of different species. When "BB" interactions were smaller than the interaction between "AA" particles the formation of particles of an specific specie was determined by the individual interactions of each specie, *i.e.* strong "BB" interactions produced more "B" particles. This issue was observed in all the systems regardless the simulation temperature.

On the other hand, if the cross interaction "AB" was stronger that the "AA" and "BB" interactions then creation of B particles, in general, was favored. From the results it was also possible to observe that adsorption on the walls was determined by the number of particles created close to the walls with the formation of high peaks and strong fluid structures of the dominated specie in the mixture.

Finally, we can say that rich phases of one particular specie of particles can be controlled by strong or weak interaction of this specie with the walls, *e.g.* strong wall - "B" particle interactions produced that those particles were more abundant in the system.

---

1. P. J. Barrie, *ANN R NMR S.* **41** (2000) 265.

2. J. A. Duffy and M. A. Alam, *Langmuir.* **16** (2000) 9513.

3. D. G. Jones and H. M. Fretwell, *J Phys-Condens Mat.* **15** (2003) 4709.

4. M. Sliwinska-Bartkowiak *et al., Stud Surf Sci Catal.* **128** (2000) 141.

5. S. Varga *et al., J. Colloid Interf Sci.* **227** (2000) 223.

6. A. Chrzanowska, *J. Comput Phys.* **191** (2003) 265.

7. M. B. Sweatman, A. A. Atamas, and J. M. Leyssale, *Journal OF Chemical Physics.* **128** (2008) 064102.

8. M. B. Sweatman and N. Quirke, *Molecular Simulation.* **31** (2005) 667.

9. T. Kaneko, T. Mima, and K. Yasuoka, *Chemical Physics Letters.* **490** (2010) 165.

10. M. Schmidt, A. Fortini, and M. Dijkstra, *Journal of Physics-Condensed Matter.* **16** (2004) S4159.

11. E. Diaz-Herrera, J. A. Moreno-Razo, and G. Ramirez-Santiago, *Physical Review E.* **70** (2004) 051601.

12. B. Coasne *et al.*, *Journal of Physical Chemistry B*. **113** (2009) 13874.

13. H. Dominguez, M. P. Allen, and R. Evans, *Molec. Phys.* **96** (1999) 209.

14. M. Lupkowski and F. van Swol, *J. Chem. Phys.* **93** (1990) 737.

15. J. E. Hug, F. van Swol and C. F. Zukoski, *Langmuir* **11** (1995) 111.

16. M. Miyahara and K. E. Gubbins, *J. Chem. Phys.* **106** (1997) 2865.

17. M. W. Madox and K. E. Gubbins, *J. Chem. Phys.* **107** (1997) 9659.

18. J. K. Johnson, A. Z. Panagiotopoulos, and K. E.Gubbins, *Molec. Phys.* **81** (1994) 717.

19. M. Lisal, J. K. Brennan, and W. R. Smith, *J. Chem. Phys.* **124** (2006) 064712.

20. C. H. Turner, J. K. Johnson, and K. E. Gubbins, *J. Chem. Phys.* **114** (2001) 1851.

21. N. Hansen, S. Jakobtorweihen, and F. J. Keil, *J. Chem. Phys.* **122** (2005) 164705.

22. S. Jakobtorweihen, N. Hansen, and F. J. Keil, *J. Chem. Phys.* **125** (2006) 224709.

23. K. E. Gubbins, Y-C. Liu, J. D. Moore, and J. C. Palmer, *Phys. Chem. Chem. Phys.* **13** (2011) 58.

24. C. H. Turner *et al.*, *Molecular Simulation.* **34** (2008) 119.

25. M. P. Allen and D. J. Tildesley, *Computer Simulations of Liquids* (Claredon Press, Oxford, 1993).